

A Search for the Associated Production of the Standard-Model Higgs Boson in the All-Hadronic Channel

- T. Aaltonen,²⁴ J. Adelman,¹⁴ T. Akimoto,⁵⁶ M.G. Albrow,¹⁸ B. Álvarez González,¹² S. Amerio^u,⁴⁴ D. Amidei,³⁵
 A. Anastassov,³⁹ A. Annovi,²⁰ J. Antos,¹⁵ G. Apollinari,¹⁸ A. Apresyan,⁴⁹ T. Arisawa,⁵⁸ A. Artikov,¹⁶
 W. Ashmanskas,¹⁸ A. Attal,⁴ A. Aurisano,⁵⁴ F. Azfar,⁴³ P. Azzurri^s,⁴⁷ W. Badgett,¹⁸ A. Barbaro-Galtieri,²⁹
 V.E. Barnes,⁴⁹ B.A. Barnett,²⁶ V. Bartsch,³¹ G. Bauer,³³ P.-H. Beauchemin,³⁴ F. Bedeschi,⁴⁷ P. Bednar,¹⁵
 D. Beecher,³¹ S. Behari,²⁶ G. Bellettini^q,⁴⁷ J. Bellinger,⁶⁰ D. Benjamin,¹⁷ A. Beretvas,¹⁸ J. Beringer,²⁹ A. Bhatti,⁵¹
 M. Binkley,¹⁸ D. Bisello^u,⁴⁴ I. Bizjak,³¹ R.E. Blair,² C. Blocker,⁷ B. Blumenfeld,²⁶ A. Bocci,¹⁷ A. Bodek,⁵⁰
 V. Boisvert,⁵⁰ G. Bolla,⁴⁹ D. Bortoletto,⁴⁹ J. Boudreau,⁴⁸ A. Boveia,¹¹ B. Brau,¹¹ A. Bridgeman,²⁵ L. Brigliadori,⁴⁴
 C. Bromberg,³⁶ E. Brubaker,¹⁴ J. Budagov,¹⁶ H.S. Budd,⁵⁰ S. Budd,²⁵ K. Burkett,¹⁸ G. Busetto^u,⁴⁴ P. Bussey^x,²²
 A. Buzatu,³⁴ K. L. Byrum,² S. Cabrera^p,¹⁷ C. Calancha,³² M. Campanelli,³⁶ M. Campbell,³⁵ F. Canelli,¹⁸
 A. Canepa,⁴⁶ D. Carlsmith,⁶⁰ R. Carosi,⁴⁷ S. Carrillo^j,¹⁹ S. Carron,³⁴ B. Casal,¹² M. Casarsa,¹⁸ A. Castro^t,⁶
 P. Catastini^r,⁴⁷ D. Cauz^w,⁵⁵ V. Cavaliere^r,⁴⁷ M. Cavalli-Sforza,⁴ A. Cerri,²⁹ L. Cerritoⁿ,³¹ S.H. Chang,²⁸
 Y.C. Chen,¹ M. Chertok,⁸ G. Chiarelli,⁴⁷ G. Chlachidze,¹⁸ F. Chlebana,¹⁸ K. Cho,²⁸ D. Chokheli,¹⁶ J.P. Chou,²³
 G. Choudalakis,³³ S.H. Chuang,⁵³ K. Chung,¹³ W.H. Chung,⁶⁰ Y.S. Chung,⁵⁰ C.I. Ciobanu,⁴⁵ M.A. Ciocci^r,⁴⁷
 A. Clark,²¹ D. Clark,⁷ G. Compostella,⁴⁴ M.E. Convery,¹⁸ J. Conway,⁸ K. Copic,³⁵ M. Cordelli,²⁰ G. Cortiana^u,⁴⁴
 D.J. Cox,⁸ F. Crescioli^q,⁴⁷ C. Cuencia Almenar^p,⁸ J. Cuevas^m,¹² R. Culbertson,¹⁸ J.C. Cully,³⁵ D. Dagenhart,¹⁸
 M. Datta,¹⁸ T. Davies,²² P. de Barbaro,⁵⁰ S. De Cecco,⁵² A. Deisher,²⁹ G. De Lorenzo,⁴ M. Dell'Orso^q,⁴⁷
 C. Deluca,⁴ L. Demortier,⁵¹ J. Deng,¹⁷ M. Deninno,⁶ P.F. Derwent,¹⁸ G.P. di Giovanni,⁴⁵ C. Dionisi^v,⁵²
 B. Di Ruzza^w,⁵⁵ J.R. Dittmann,⁵ M. D'Onofrio,⁴ S. Donati^q,⁴⁷ P. Dong,⁹ J. Donini,⁴⁴ T. Dorigo,⁴⁴ S. Dube,⁵³
 J. Efron,⁴⁰ A. Elagin,⁵⁴ R. Erbacher,⁸ D. Errede,²⁵ S. Errede,²⁵ R. Eusebi,¹⁸ H.C. Fang,²⁹ S. Farrington,⁴³
 W.T. Fedorko,¹⁴ R.G. Feild,⁶¹ M. Feindt,²⁷ J.P. Fernandez,³² C. Ferrazza^s,⁴⁷ R. Field,¹⁹ G. Flanagan,⁴⁹ R. Forrest,⁸
 M. Franklin,²³ J.C. Freeman,¹⁸ I. Furic,¹⁹ M. Gallinaro,⁵² J. Galyardt,¹³ F. Garberson,¹¹ J.E. Garcia,⁴⁷
 A.F. Garfinkel,⁴⁹ K. Genser,¹⁸ H. Gerberich,²⁵ D. Gerdes,³⁵ A. Gessler,²⁷ S. Giagu^v,⁵² V. Giakoumopoulou,³
 P. Giannetti,⁴⁷ K. Gibson,⁴⁸ J.L. Gimmell,⁵⁰ C.M. Ginsburg,¹⁸ N. Giokaris,³ M. Giordani^w,⁵⁵ P. Giromini,²⁰
 M. Giunta^q,⁴⁷ G. Giurgiu,²⁶ V. Glagolev,¹⁶ D. Glenzinski,¹⁸ M. Gold,³⁸ N. Goldschmidt,¹⁹ A. Golossanov,¹⁸
 G. Gomez,¹² G. Gomez-Ceballos,³³ M. Goncharov,⁵⁴ O. González,³² I. Gorelov,³⁸ A.T. Goshaw,¹⁷ K. Goulianatos,⁵¹
 A. Gresel^u,⁴⁴ S. Grinstein,²³ C. Grossi-Pilcher,¹⁴ R.C. Group,¹⁸ U. Grundler,²⁵ J. Guimaraes da Costa,²³
 Z. Gunay-Unalan,³⁶ C. Haber,²⁹ K. Hahn,³³ S.R. Hahn,¹⁸ E. Halkiadakis,⁵³ B.-Y. Han,⁵⁰ J.Y. Han,⁵⁰ R. Handler,⁶⁰
 F. Happacher,²⁰ K. Hara,⁵⁶ D. Hare,⁵³ M. Hare,⁵⁷ S. Harper,⁴³ R.F. Harr,⁵⁹ R.M. Harris,¹⁸ M. Hartz,⁴⁸
 K. Hatakeyama,⁵¹ J. Hauser,⁹ C. Hays,⁴³ M. Heck,²⁷ A. Heijboer,⁴⁶ B. Heinemann,²⁹ J. Heinrich,⁴⁶ C. Henderson,³³
 M. Herndon,⁶⁰ J. Heuser,²⁷ S. Hewamanage,⁵ D. Hidas,¹⁷ C.S. Hill^c,¹¹ D. Hirschbuehl,²⁷ A. Hocker,¹⁸ S. Hou,¹
 M. Houlden,³⁰ S.-C. Hsu,¹⁰ B.T. Huffman,⁴³ R.E. Hughes,⁴⁰ U. Husemann,⁶¹ J. Huston,³⁶ J. Incandela,¹¹
 G. Introzzi,⁴⁷ M. Iori^v,⁵² A. Ivanov,⁸ E. James,¹⁸ B. Jayatilaka,¹⁷ E.J. Jeon,²⁸ M.K. Jha,⁶ S. Jindariani,¹⁸
 W. Johnson,⁸ M. Jones,⁴⁹ K.K. Joo,²⁸ S.Y. Jun,¹³ J.E. Jung,²⁸ T.R. Junk,¹⁸ T. Kamon,⁵⁴ D. Kar,¹⁹ P.E. Karchin,⁵⁹
 Y. Kato,⁴² R. Kephart,¹⁸ J. Keung,⁴⁶ V. Khotilovich,⁵⁴ B. Kilminster,⁴⁰ D.H. Kim,²⁸ H.S. Kim,²⁸ J.E. Kim,²⁸
 M.J. Kim,²⁰ S.B. Kim,²⁸ S.H. Kim,⁵⁶ Y.K. Kim,¹⁴ N. Kimura,⁵⁶ L. Kirsch,⁷ S. Klimentko,¹⁹ B. Knuteson,³³
 B.R. Ko,¹⁷ S.A. Koay,¹¹ K. Kondo,⁵⁸ D.J. Kong,²⁸ J. Konigsberg,¹⁹ A. Korytov,¹⁹ A.V. Kotwal,¹⁷ M. Kreps,²⁷
 J. Kroll,⁴⁶ D. Krop,¹⁴ N. Krummack,⁵ M. Kruse,¹⁷ V. Krutelyov,¹¹ T. Kubo,⁵⁶ T. Kuhr,²⁷ N.P. Kulkarni,⁵⁹
 M. Kurata,⁵⁶ Y. Kusakabe,⁵⁸ S. Kwang,¹⁴ A.T. Laasanen,⁴⁹ S. Lami,⁴⁷ S. Lammel,¹⁸ M. Lancaster,³¹ R.L. Lander,⁸
 K. Lannon,⁴⁰ A. Lath,⁵³ G. Latino^r,⁴⁷ I. Lazzizzera^u,⁴⁴ T. LeCompte,² E. Lee,⁵⁴ S.W. Lee^o,⁵⁴ S. Leone,⁴⁷
 J.D. Lewis,¹⁸ C.S. Lin,²⁹ J. Linacre,⁴³ M. Lindgren,¹⁸ E. Lipeles,¹⁰ A. Lister,⁸ D.O. Litvintsev,¹⁸ C. Liu,⁴⁸ T. Liu,¹⁸
 N.S. Lockyer,⁴⁶ A. Loginov,⁶¹ M. Loretⁱ^u,⁴⁴ L. Lovas,¹⁵ R.-S. Lu,¹ D. Lucchesi^u,⁴⁴ J. Lueck,²⁷ C. Luci^v,⁵²
 P. Lujan,²⁹ P. Lukens,¹⁸ G. Lungu,⁵¹ L. Lyons,⁴³ J. Lys,²⁹ R. Lysak,¹⁵ E. Lytken,⁴⁹ P. Mack,²⁷ D. MacQueen,³⁴
 R. Madrak,¹⁸ K. Maeshima,¹⁸ K. Makhoul,³³ T. Maki,²⁴ P. Maksimovic,²⁶ S. Malde,⁴³ S. Malik,³¹ G. Manca^y,³⁰
 A. Manousakis-Katsikakis,³ F. Margaroli,⁴⁹ C. Marino,²⁷ C.P. Marino,²⁵ A. Martin,⁶¹ V. Martinⁱ,²² M. Martínez,⁴
 R. Martínez-Ballarín,³² T. Maruyama,⁵⁶ P. Mastrandrea,⁵² T. Masubuchi,⁵⁶ M.E. Mattson,⁵⁹ P. Mazzanti,⁶
 K.S. McFarland,⁵⁰ P. McIntyre,⁵⁴ R. McNulty^h,³⁰ A. Mehta,³⁰ P. Mehtala,²⁴ A. Menzione,⁴⁷ P. Merkel,⁴⁹
 C. Mesropian,⁵¹ T. Miao,¹⁸ N. Miladinovic,⁷ R. Miller,³⁶ C. Mills,²³ M. Milnik,²⁷ A. Mitra,¹ G. Mitselmakher,¹⁹
 H. Miyake,⁵⁶ N. Moggi,⁶ C.S. Moon,²⁸ R. Moore,¹⁸ M.J. Morello^q,⁴⁷ J. Morlok,²⁷ P. Movilla Fernandez,¹⁸

J. Mülmenstädt,²⁹ A. Mukherjee,¹⁸ Th. Muller,²⁷ R. Mumford,²⁶ P. Murat,¹⁸ M. Mussini^{t, 6} J. Nachtman,¹⁸ Y. Nagai,⁵⁶ A. Nagano,⁵⁶ J. Naganoma,⁵⁸ K. Nakamura,⁵⁶ I. Nakano,⁴¹ A. Napier,⁵⁷ V. Necula,¹⁷ C. Neu,⁴⁶ M.S. Neubauer,²⁵ J. Nielsen^{e, 29} L. Nodulman,² M. Norman,¹⁰ O. Norniella,²⁵ E. Nurse,³¹ L. Oakes,⁴³ S.H. Oh,¹⁷ Y.D. Oh,²⁸ I. Oksuzian,¹⁹ T. Okusawa,⁴² R. Orava,²⁴ K. Osterberg,²⁴ S. Pagan Griso^{u, 44} C. Pagliarone,⁴⁷ E. Palencia,¹⁸ V. Papadimitriou,¹⁸ A. Papaikonomou,²⁷ A.A. Paramonov,¹⁴ B. Parks,⁴⁰ S. Pashapour,³⁴ J. Patrick,¹⁸ G. Paulettaw,⁵⁵ M. Paulini,¹³ C. Paus,³³ D.E. Pellett,⁸ A. Penzo,⁵⁵ T.J. Phillips,¹⁷ G. Piacentino,⁴⁷ E. Pianori,⁴⁶ L. Pinera,¹⁹ K. Pitts,²⁵ C. Plager,⁹ L. Pondrom,⁶⁰ O. Poukhov*,¹⁶ N. Pounder,⁴³ F. Prakoshyn,¹⁶ A. Pronko,¹⁸ J. Proudfoot,² F. Ptahos^{g, 18} E. Pueschel,¹³ G. Punzi^{q, 47} J. Pursley,⁶⁰ J. Rademacker^{c, 43} A. Rahaman,⁴⁸ V. Ramakrishnan,⁶⁰ N. Ranjan,⁴⁹ I. Redondo,³² B. Reisert,¹⁸ V. Rekovic,³⁸ P. Renton,⁴³ M. Rescigno,⁵² S. Richter,²⁷ F. Rimondi^{t, 6} L. Ristori,⁴⁷ A. Robson,²² T. Rodrigo,¹² T. Rodriguez,⁴⁶ E. Rogers,²⁵ S. Rolli,⁵⁷ R. Roser,¹⁸ M. Rossi,⁵⁵ R. Rossin,¹¹ P. Roy,³⁴ A. Ruiz,¹² J. Russ,¹³ V. Rusu,¹⁸ H. Saarikko,²⁴ A. Safonov,⁵⁴ W.K. Sakumoto,⁵⁰ O. Saltó,⁴ L. Santi^{w, 55} S. Sarkar^{v, 52} L. Sartori,⁴⁷ K. Sato,¹⁸ A. Savoy-Navarro,⁴⁵ T. Scheidle,²⁷ P. Schlabach,¹⁸ A. Schmidt,²⁷ E.E. Schmidt,¹⁸ M.A. Schmidt,¹⁴ M.P. Schmidt^{†, 61} M. Schmitt,³⁹ T. Schwarz,⁸ L. Scodellaro,¹² A.L. Scott,¹¹ A. Scribano^{r, 47} F. Scuri,⁴⁷ A. Sedov,⁴⁹ S. Seidel,³⁸ Y. Seiya,⁴² A. Semenov,¹⁶ L. Sexton-Kennedy,¹⁸ A. Sfyrla,²¹ S.Z. Shalhout,⁵⁹ T. Shears,³⁰ P.F. Shepard,⁴⁸ D. Sherman,²³ M. Shimojima^{l, 56} S. Shiraishi,¹⁴ M. Shochet,¹⁴ Y. Shon,⁶⁰ I. Shreyber,³⁷ A. Sidoti,⁴⁷ P. Sinervo,³⁴ A. Sisakyan,¹⁶ A.J. Slaughter,¹⁸ J. Slaunwhite,⁴⁰ K. Sliwa,⁵⁷ J.R. Smith,⁸ F.D. Snider,¹⁸ R. Snihur,³⁴ A. Soha,⁸ S. Somalwar,⁵³ V. Sorin,³⁶ J. Spalding,¹⁸ T. Spreitzer,³⁴ P. Squillacioti^{r, 47} M. Stanitzki,⁶¹ R. St. Denis,²² B. Stelzer,⁹ O. Stelzer-Chilton,⁴³ D. Stentz,³⁹ J. Strologas,³⁸ D. Stuart,¹¹ J.S. Suh,²⁸ A. Sukhanov,¹⁹ I. Suslov,¹⁶ T. Suzuki,⁵⁶ A. Taffard^{d, 25} R. Takashima,⁴¹ Y. Takeuchi,⁵⁶ R. Tanaka,⁴¹ M. Tecchio,³⁵ P.K. Teng,¹ K. Terashi,⁵¹ J. Thom^{f, 18} A.S. Thompson,²² G.A. Thompson,²⁵ E. Thomson,⁴⁶ P. Tipton,⁶¹ V. Tiwari,¹³ S. Tkaczyk,¹⁸ D. Toback,⁵⁴ S. Tokar,¹⁵ K. Tollefson,³⁶ T. Tomura,⁵⁶ D. Tonelli,¹⁸ S. Torre,²⁰ D. Torretta,¹⁸ P. Totaro^{w, 55} S. Tourneur,⁴⁵ Y. Tu,⁴⁶ N. Turini^{r, 47} F. Ukegawa,⁵⁶ S. Vallecorsa,²¹ N. van Remortel^{a, 24} A. Varganov,³⁵ E. Vataga^{s, 47} F. Vázquez^{j, 19} G. Velev,¹⁸ C. Vellidis,³ V. Veszprenyi,⁴⁹ M. Vidal,³² R. Vidal,¹⁸ I. Vila,¹² R. Vilar,¹² T. Vine,³¹ M. Vogel,³⁸ I. Volobouev^{o, 29} G. Volpi^{q, 47} F. Würthwein,¹⁰ P. Wagner,² R.G. Wagner,² R.L. Wagner,¹⁸ J. Wagner-Kuhr,²⁷ W. Wagner,²⁷ T. Wakisaka,⁴² R. Wallny,⁹ S.M. Wang,¹ A. Warburton,³⁴ D. Waters,³¹ M. Weinberger,⁵⁴ W.C. Wester III,¹⁸ B. Whitehouse,⁵⁷ D. Whiteson^{d, 46} A.B. Wicklund,² E. Wicklund,¹⁸ G. Williams,³⁴ H.H. Williams,⁴⁶ P. Wilson,¹⁸ B.L. Winer,⁴⁰ P. Wittich^{f, 18} S. Wolbers,¹⁸ C. Wolfe,¹⁴ T. Wright,³⁵ X. Wu,²¹ S.M. Wynne,³⁰ S. Xie,³³ A. Yagil,¹⁰ K. Yamamoto,⁴² J. Yamaoka,⁵³ U.K. Yang^{k, 14} Y.C. Yang,²⁸ W.M. Yao,²⁹ G.P. Yeh,¹⁸ J. Yoh,¹⁸ K. Yorita,¹⁴ T. Yoshida,⁴² G.B. Yu,⁵⁰ I. Yu,²⁸ S.S. Yu,¹⁸ J.C. Yun,¹⁸ L. Zanello^{v, 52} A. Zanetti,⁵⁵ I. Zaw,²³ X. Zhang,²⁵ Y. Zheng^{b, 9} and S. Zucchelli^{t, 6}

(CDF Collaboration[†])

¹Institute of Physics, Academia Sinica, Taipei, Taiwan 11529, Republic of China

²Argonne National Laboratory, Argonne, Illinois 60439

³University of Athens, 157 71 Athens, Greece

⁴Institut de Fisica d'Altes Energies, Universitat Autònoma de Barcelona, E-08193, Bellaterra (Barcelona), Spain

⁵Baylor University, Waco, Texas 76798

⁶Istituto Nazionale di Fisica Nucleare Bologna, ^tUniversity of Bologna, I-40127 Bologna, Italy

⁷Brandeis University, Waltham, Massachusetts 02254

⁸University of California, Davis, Davis, California 95616

⁹University of California, Los Angeles, Los Angeles, California 90024

¹⁰University of California, San Diego, La Jolla, California 92093

¹¹University of California, Santa Barbara, Santa Barbara, California 93106

¹²Instituto de Fisica de Cantabria, CSIC-University of Cantabria, 39005 Santander, Spain

¹³Carnegie Mellon University, Pittsburgh, PA 15213

¹⁴Enrico Fermi Institute, University of Chicago, Chicago, Illinois 60637

¹⁵Comenius University, 842 48 Bratislava, Slovakia; Institute of Experimental Physics, 040 01 Kosice, Slovakia

¹⁶Joint Institute for Nuclear Research, RU-141980 Dubna, Russia

¹⁷Duke University, Durham, North Carolina 27708

¹⁸Fermi National Accelerator Laboratory, Batavia, Illinois 60510

¹⁹University of Florida, Gainesville, Florida 32611

²⁰Laboratori Nazionali di Frascati, Istituto Nazionale di Fisica Nucleare, I-00044 Frascati, Italy

²¹University of Geneva, CH-1211 Geneva 4, Switzerland

²²Glasgow University, Glasgow G12 8QQ, United Kingdom

²³Harvard University, Cambridge, Massachusetts 02138

- ²⁴*Division of High Energy Physics, Department of Physics,
University of Helsinki and Helsinki Institute of Physics, FIN-00014, Helsinki, Finland*
- ²⁵*University of Illinois, Urbana, Illinois 61801*
- ²⁶*The Johns Hopkins University, Baltimore, Maryland 21218*
- ²⁷*Institut für Experimentelle Kernphysik, Universität Karlsruhe, 76128 Karlsruhe, Germany*
- ²⁸*Center for High Energy Physics: Kyungpook National University,
Daegu 702-701, Korea; Seoul National University, Seoul 151-742,
Korea; Sungkyunkwan University, Suwon 440-746,
Korea; Korea Institute of Science and Technology Information, Daejeon,
305-806, Korea; Chonnam National University, Gwangju, 500-757, Korea*
- ²⁹*Ernest Orlando Lawrence Berkeley National Laboratory, Berkeley, California 94720*
- ³⁰*University of Liverpool, Liverpool L69 7ZE, United Kingdom*
- ³¹*University College London, London WC1E 6BT, United Kingdom*
- ³²*Centro de Investigaciones Energeticas Medioambientales y Tecnologicas, E-28040 Madrid, Spain*
- ³³*Massachusetts Institute of Technology, Cambridge, Massachusetts 02139*
- ³⁴*Institute of Particle Physics: McGill University, Montréal,
Canada H3A 2T8; and University of Toronto, Toronto, Canada M5S 1A7*
- ³⁵*University of Michigan, Ann Arbor, Michigan 48109*
- ³⁶*Michigan State University, East Lansing, Michigan 48824*
- ³⁷*Institution for Theoretical and Experimental Physics, ITEP, Moscow 117259, Russia*
- ³⁸*University of New Mexico, Albuquerque, New Mexico 87131*
- ³⁹*Northwestern University, Evanston, Illinois 60208*
- ⁴⁰*The Ohio State University, Columbus, Ohio 43210*
- ⁴¹*Okayama University, Okayama 700-8530, Japan*
- ⁴²*Osaka City University, Osaka 588, Japan*
- ⁴³*University of Oxford, Oxford OX1 3RH, United Kingdom*
- ⁴⁴*Istituto Nazionale di Fisica Nucleare, Sezione di Padova-Trento, ^aUniversity of Padova, I-35131 Padova, Italy*
- ⁴⁵*LPNHE, Université Pierre et Marie Curie/IN2P3-CNRS, UMR7585, Paris, F-75252 France*
- ⁴⁶*University of Pennsylvania, Philadelphia, Pennsylvania 19104*
- ⁴⁷*Istituto Nazionale di Fisica Nucleare Pisa, ^aUniversity of Pisa,
^rUniversity of Siena and ^sScuola Normale Superiore, I-56127 Pisa, Italy*
- ⁴⁸*University of Pittsburgh, Pittsburgh, Pennsylvania 15260*
- ⁴⁹*Purdue University, West Lafayette, Indiana 47907*
- ⁵⁰*University of Rochester, Rochester, New York 14627*
- ⁵¹*The Rockefeller University, New York, New York 10021*
- ⁵²*Istituto Nazionale di Fisica Nucleare, Sezione di Roma 1,
^vSapienza Università di Roma, I-00185 Roma, Italy*
- ⁵³*Rutgers University, Piscataway, New Jersey 08855*
- ⁵⁴*Texas A&M University, College Station, Texas 77843*
- ⁵⁵*Istituto Nazionale di Fisica Nucleare Trieste/ Udine, ^wUniversity of Trieste/ Udine, Italy*
- ⁵⁶*University of Tsukuba, Tsukuba, Ibaraki 305, Japan*
- ⁵⁷*Tufts University, Medford, Massachusetts 02155*
- ⁵⁸*Waseda University, Tokyo 169, Japan*
- ⁵⁹*Wayne State University, Detroit, Michigan 48201*
- ⁶⁰*University of Wisconsin, Madison, Wisconsin 53706*
- ⁶¹*Yale University, New Haven, Connecticut 06520*

We report on a search for the standard-model Higgs boson in $p\bar{p}$ collisions at $\sqrt{s} = 1.96$ TeV using an integrated luminosity of 2.0 fb^{-1} . We look for production of the Higgs boson decaying to a pair of bottom quarks in association with a vector boson V (W or Z) decaying to quarks, resulting in a four-jet final state. Two of the jets are required to have secondary vertices consistent with B-hadron decays. We set the first 95% confidence level upper limit on the VH production cross section with $V(\rightarrow q\bar{q}/q\bar{q}')H(\rightarrow b\bar{b})$ decay for Higgs boson masses of 100–150 GeV/c^2 using data from Run II at the Fermilab Tevatron. For $m_H = 120 \text{ GeV}/c^2$, we exclude cross sections larger than 38 times the standard-model prediction.

PACS numbers: 14.65.Ha, 13.85.Ni, 13.85.Qk, 12.15.Ff

^{*}Deceased
[†]Deceased

[‡]With visitors from ^aUniversiteit Antwerpen, B-2610 Antwerp,

The standard model (SM) of elementary particle physics includes a scalar Higgs (H) boson to explain the origins of electroweak-symmetry breaking [1, 2]. Direct searches for the Higgs scalar boson at the LEP collider [3] have constrained the Higgs boson mass (m_H) to be greater than $114.4 \text{ GeV}/c^2$ at 95% confidence level (CL). For Higgs boson masses above this limit, the CDF and DØ experiments at the Tevatron collider are currently performing the most sensitive searches [4]. Global fits to electroweak data [5] indicate a light SM Higgs boson, excluding $m_H > 154 \text{ GeV}/c^2$ at 95% CL. Searches for a low-mass Higgs boson are thus particularly relevant. For $m_H < 135 \text{ GeV}/c^2$, the dominant decay mode is $H \rightarrow b\bar{b}$ [6]. While the dominant production modes are direct $gg \rightarrow H$ and $q\bar{q} \rightarrow H$, the $b\bar{b}$ signature in this channel is overwhelmed by background from QCD $b\bar{b}$ production. Searches for events where the Higgs boson is produced in association with a vector boson ($V = W$ or Z) are more promising. The VH associated production cross section is smaller by an order of magnitude than for direct production, but identification of the accompanying vector boson reduces the QCD background, making searches for VH the most sensitive ones at low Higgs-boson mass.

So far, Tevatron Run II searches [7, 8] have used signatures where the V decays to leptons. In this Letter we report on an analysis of the channel in which the V decays to a $q\bar{q}$ pair resulting in two jets. Using data from 2.0 fb^{-1} of integrated luminosity collected by the CDF experiment, we search for four-jet events compatible with the VH decay. While this channel has a large QCD background, it benefits from the combined cross sections of ZH and WH production as well as the large $V \rightarrow q\bar{q}/qq'$ branching ratio of about 70% [9]. An analysis of this channel in Run I of the Tevatron [10] suggests strong potential. This Letter presents the first analysis of this channel using data from Run II of the Tevatron; we find that uncertainties on the dominant background are larger than had been anticipated [11].

The CDF II detector [12, 13] consists of a cylindrical

magnetic spectrometer surrounded by sampling calorimeters used to measure the energies of the jets. Charged particle tracking is performed with silicon microstrip detectors surrounded by a large cylindrical multilayer drift chamber, immersed in a solenoidal magnetic field. Planar drift chambers surround the calorimeters to detect muons.

The data were collected using a three-level multi-jet online event selection (trigger) [14], originally designed for hadronic top decays. To trigger a jet, in the first stage (level 1) a single calorimeter tower was required with a transverse energy (E_T) [15] of at least $10(20) \text{ GeV}$ for the data from the first (second) fb^{-1} of integrated luminosity. At level 2, clusters of contiguous calorimeter towers were identified and a fast online cluster energy measurement was performed. Four clusters with $E_T > 15 \text{ GeV}$ were required. Additionally, the total transverse energy, $\sum E_T$, was required to exceed $125 (175) \text{ GeV}$ for the first 0.4 (last 1.6) fb^{-1} to reduce backgrounds from soft QCD jets. The thresholds were increased in the later periods to maintain an acceptable trigger rate as the instantaneous luminosity increased over time. No rejection is made by the level 3 trigger.

The trigger efficiency for the VH signal is estimated using a combination of PYTHIA [16] simulation and data. Interaction of the final-state particles with the CDF II detector is described by a GEANT-based detector simulation [17]. The data used to measure the efficiency were collected by triggers which required a single jet with E_T greater than 20 or 50 GeV. Corrections to the simulated VH trigger efficiency were derived by comparing these data to the corresponding simulations. The corrections account for imperfect simulation of the soft hadron activity and jet finding in the trigger algorithm and differences in the energy scale at the trigger level between data and simulation. These corrections result in a relative reduction of the estimated efficiency for the VH signal by $\sim 20\%$. A systematic uncertainty of 7% (relative) on the trigger efficiency is derived by comparing the corrections found in data with different single-jet energy thresholds, and in different data periods. The uncertainty of the trigger acceptance due to initial- and final-state radiation, the jet energy scale and the parton distribution functions are handled separately. The overall trigger efficiency for the VH signal (with $m_H = 120 \text{ GeV}/c^2$) is $33 \pm 2\% (17 \pm 1\%)$ for the $\sum E_T$ threshold of $125(175) \text{ GeV}$.

In the final offline selection, jets are identified as energy depositions in the calorimeters by the JETCLU [18] algorithm with a clustering radius of 0.4 in azimuth-pseudorapidity space. The reconstructed jet energies are corrected to give the best estimate of the energy of each quark, including effects of calorimeter response, multiple $p\bar{p}$ interactions, the underlying event, and energy deposited outside the clustered jet [19]. Jets originating from b -quarks are identified, or ‘ b -tagged’, by the SECVTX

Belgium, ^bChinese Academy of Sciences, Beijing 100864, China,
^cUniversity of Bristol, Bristol BS8 1TL, United Kingdom,
^dUniversity of California Irvine, Irvine, CA 92697, ^eUniversity of California Santa Cruz, Santa Cruz, CA 95064, ^fCornell University, Ithaca, NY 14853, ^gUniversity of Cyprus, Nicosia CY-1678, Cyprus, ^hUniversity College Dublin, Dublin 4, Ireland, ⁱUniversity of Edinburgh, Edinburgh EH9 3JZ, United Kingdom, ^jUniversidad Iberoamericana, Mexico D.F., Mexico, ^kUniversity of Manchester, Manchester M13 9PL, England, ^lNagasaki Institute of Applied Science, Nagasaki, Japan, ^mUniversity de Oviedo, E-33007 Oviedo, Spain, ⁿQueen Mary, University of London, London, E1 4NS, England, ^oTexas Tech University, Lubbock, TX 79409, ^pIFIC(CSIC-Universitat de Valencia), 46071 Valencia, Spain, ^xRoyal Society of Edinburgh/Scottish Executive Support Research Fellow, ^yIstituto Nazionale di Fisica Nucleare, Sezione di Cagliari, 09042 Monserrato (Cagliari), Italy

[20] algorithm, which searches for a secondary vertex that results from the displaced decay of a B-hadron.

Events compatible with the $VH \rightarrow qqbb$ signature are selected by requiring at least four jets with $|\eta| < 2.4$ and $E_T > 15$ GeV in which exactly two of the jets are b -tagged. The invariant mass of the b -tagged jets, m_{bb} , is required to exceed $75\text{ GeV}/c^2$. The invariant mass of the remaining leading two q jets, m_{qq} , is required to be compatible with the W or Z mass: $35 < m_{qq} < 120$ GeV/c^2 . The di-jet mass resolution in the relevant invariant mass range is of the order of $15\text{ GeV}/c^2$, so the WH and ZH channels cannot be distinguished. We refer to this as the *signal* region; see Fig. 1. Events in other regions of the (m_{bb}, m_{qq}) plane and events with at least one b -tag are used to model the QCD background to the $VH \rightarrow qqbb$ signature. Events with identified isolated leptons are removed from the sample to eliminate overlap with leptonic W, Z decay channels and reduce the background from $t\bar{t}$. The combined trigger and selection efficiency for $VH \rightarrow qqbb$ events for the entire data-taking period varies from $\sim 1\%$ to $\sim 4\%$ for Higgs boson masses between 100 and 150 GeV/c^2 .

The dominant background to the $qqbb$ final state is QCD multijet production. In order to distinguish between signal and background events, we use the log-likelihood ratio

$$Q = \log \left(\frac{P(\mathbf{x}|WH) + P(\mathbf{x}|ZH)}{P(\mathbf{x}|QCD)} \right),$$

where \mathbf{x} is the vector of measured jet momenta of the four highest E_T jets, and $P(\mathbf{x}|WH)$, $P(\mathbf{x}|ZH)$ and $P(\mathbf{x}|QCD)$ are the likelihoods of observing the event \mathbf{x} for the WH , ZH and QCD processes respectively. The likelihoods are calculated by convoluting the differential cross section as a function of the incoming and outgoing quark momenta for the processes with parameterized detector resolution functions, and numerically integrating over the unmeasured magnitudes of the quark momenta [21]. $P(\mathbf{x}|process)$ is defined as

$$\begin{aligned} P(\mathbf{x}|process) &= \int d\Phi |\mathcal{M}_{\text{process}}|^2 P_{\text{tot}} \\ &\times \prod_{j=1\dots 4} T(E_{\text{jet}}^j | E_{\text{quark}}^j) f_p f_{\bar{p}}, \end{aligned}$$

where $d\Phi$ is the phase space of the unmeasured incoming and outgoing quark momenta, \mathcal{M} is the matrix element, P_{tot} is the probability density of the transverse momentum of the process described by the matrix element, $T(E_{\text{jet}} | E_{\text{quark}})$ is a transfer function which parameterizes the probability to measure a quark of energy E_{quark} as a jet with energy E_{jet} , and f_p and $f_{\bar{p}}$ are the parton distribution functions [22] for the proton and anti-proton. The jet directions are assumed to be measured perfectly,

so that the integration is over the magnitudes of the four quark momenta.

The matrix elements for WH and ZH are numerically calculated by the ALPGEN [23] simulation. The matrix element $\mathcal{M}_{gg \rightarrow ggbb}$ is used to describe the dominant background process and is calculated by the MADGRAPH [24] simulation. However, these matrix elements do not describe initial state radiation, which could result in non-zero total transverse momentum of the VH system. The probability density of the transverse momentum, P_{tot} , is extracted from simulated PYTHIA events that include radiation. The likelihoods $P(x|ZH)$, $P(x|WH)$, and $P(x|QCD)$ are computed for m_H between 100 and 150 GeV/c^2 with 10 GeV/c^2 intervals; values at intermediate mass points are interpolated. The transfer functions were extracted from simulated events separately for b -jets and light-quark jets, accounting for the reduced jet energy for b -jets due to semileptonic decays.

Models of the Q likelihood ratio distribution are constructed for both signal and background events. Backgrounds from $t\bar{t}$, single top, and diboson production are modeled by PYTHIA. ALPGEN is used to simulate the leading-order multiparton final state for the W with heavy-flavor jets background, while the hadronization and parton showering are modeled by PYTHIA. Systematic uncertainties in the signal acceptance, which includes trigger and selection efficiency, and the shape of the signal in Q come from rates of initial- and final-state radiation, the jet energy scale, the parton distribution functions, the trigger acceptance and the b -tagging efficiency. The 7% trigger efficiency uncertainty is applied as a rate error for all simulated samples. Uncertainties in the cross sections of the background processes contribute to the systematic uncertainty in the background rate.

A model for the primary background is constructed from the data using the background-dominated sample with at least one b -tagged jet. Each of the additional jets, called a *probe* jet, is weighted by the probability for it to receive a b -tag, called the tag rate function (TRF). For an event to contribute to the background model in the signal region, the invariant mass of the tagged jet and the probe jet must exceed $75\text{ GeV}/c^2$ and the mass of the other two leading jets, m_{qq} , in the event must be between 35 and 120 GeV/c^2 . Combinations for which m_{qq} is outside this window represent an orthogonal set of probe-jets, which was used to measure the TRF. In particular, the TRF is measured on combinations where the mass of the other two jets are incompatible with the vector boson masses, $m_{qq} < 25\text{ GeV}/c^2$ or $m_{qq} > 130\text{ GeV}/c^2$ (the region labeled *tag* in Fig. 1).

The tag rate is measured as a function of four variables: the p_T of the probe jet, the number of tracks in the probe jet that traverse the silicon detector, ΔR between the probe jet and the tagged jet, and the invariant mass of the probe and the tagged jet. The TRF is implemented using a four-dimensional histogram with bin-sizes $14\text{ GeV}/c \times$

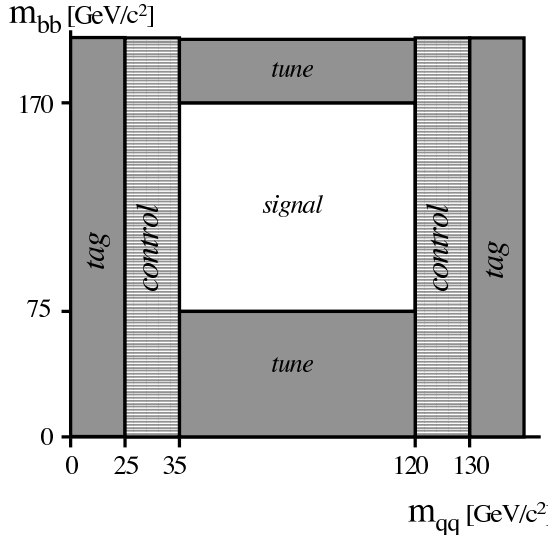


FIG. 1: Regions in the plane of m_{bb} , invariant mass of the two b -jets, and m_{qq} , invariant mass of the two other jets. The *tag* and *tune* regions are used to define and tune the tag rate function used to predict the background contribution from QCD $b\bar{b}$ production in the *signal* region. The *control* region is used to estimate a systematic uncertainty on the interpolation of the tag rate function into the *signal* region.

$2 \times 1 \times 15$ GeV/ c^2 respectively. The TRF cannot be constructed explicitly as a function of m_{qq} , as we use this variable to interpolate from the sidebands into the signal region. A small m_{qq} -dependence of the tagging rate may result from correlations between m_{qq} and properties of the b -jets that are not modeled by the TRF. The TRF is therefore further scaled by the ratio of the observed m_{qq} distribution to the predicted m_{qq} distribution in the low-mass region, $m_{bb} < 75$ GeV/ c^2 , labeled *tune* region in Fig. 1. The correction, a smooth function of m_{qq} , is of order 5%.

We consider three sources of systematic uncertainty on the shape of the Q distribution for the QCD background. The interpolation uncertainty accounts for possible differences in the TRF between the regions where it was measured (*tag*) and applied (*signal*). An alternative TRF is measured using events with $25 < m_{qq} < 35$ GeV/ c^2 or $120 < m_{qq} < 130$ GeV/ c^2 (labeled *control* in Fig. 1). The difference in the shapes of the predicted background distribution in Q for the two TRFs is treated as a systematic uncertainty. The second source is due to uncertainty in applying the m_{qq} -tuning to the *signal* region. An alternative tuning is derived using events with $m_{bb} > 170$ GeV/ c^2 , which is similarly background-dominated. Finally, we estimate a mismodeling uncertainty due to a possible limitation of the 4-dimensional TRF parameterization to describe all the quantities that affect the shape of the Q distribution. In a large simulated $t\bar{t}$ sample, we derive a TRF using events in the

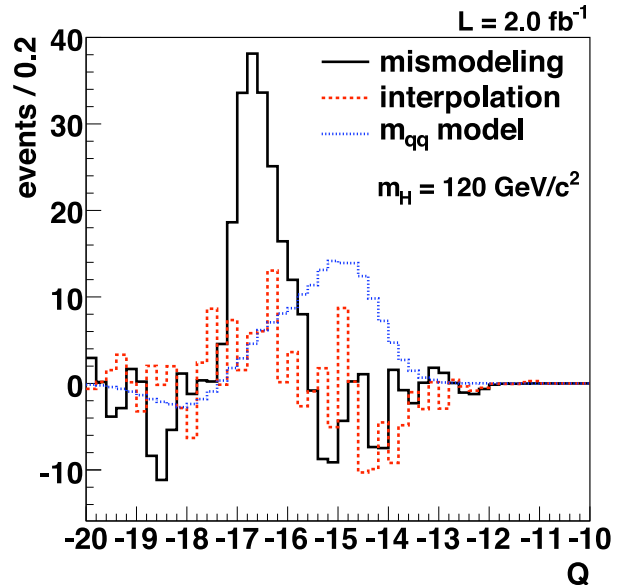


FIG. 2: Systematic uncertainties on the relative number of events expected for the QCD background model as a function of the discriminant Q , from three sources described in the text.

signal region and use it to predict the number of double-tagged events in the same *signal* region. The difference in the *signal* region between the Q distribution for double-tagged events and TRF-weighted single-tag events is used to derive the mismodeling uncertainty in the TRF method. This uncertainty describes any intrinsic failure of the TRF method to model Q distributions, independently of the details of the data sample.

The systematic shape uncertainties are shown in Fig. 2, which shows the expected deviation in the number of events within the uncertainties of the shape of the background model. In the region $Q \gtrsim -14$, where most of the Higgs boson signal would be, the systematic uncertainty on the background model is smaller than a few events per bin.

Figure 3 shows the distribution of Q for a signal ($m_H = 120$ GeV/ c^2), the background contributions, and the observed data. There is good agreement over the range of Q and no evidence of a VH signal.

To test for the presence of a VH signal in the data, a binned likelihood of the distribution of the data in Q is computed for the background-only and the signal+background hypotheses. The ratio of these likelihoods is the test statistic. The normalization of the QCD background model is a free parameter that is fit to the data. The expected distributions of the test statistic are derived from pseudo-experiments that are generated from the signal and background models, after varying them within the systematic uncertainties. All systematic uncertainties are estimated as symmetric one standard-deviation variations in the respective unknown nuisance

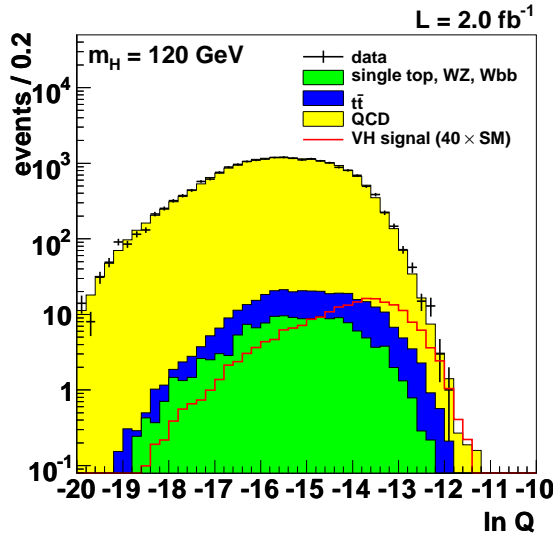


FIG. 3: Predicted and observed distribution of the Q discriminant in the signal region in 2.0 fb^{-1} of integrated luminosity. As Q is a ratio of likelihoods, its absolute scale is arbitrary.

parameter. From these distributions, limits on the VH cross section are extracted using the modified frequentist scheme [25].

Table I lists the expected and observed limits on the VH cross section expressed as a multiple of the SM cross section, σ_{SM} , for different Higgs boson masses. The observed limits agree with the expected ones. For example, for a Higgs boson mass of $120 \text{ GeV}/c^2$, the observed 95% C.L. limit is $38.2 \times \sigma_{\text{SM}}$ while the expected limit is about $40 \times \sigma_{\text{SM}}$. At higher values of m_H the sensitivity decreases due to the decreased Higgs boson production cross-section and $H \rightarrow b\bar{b}$ branching fraction. The systematic uncertainties on the background model significantly affect the sensitivity: without these, the expected limit would be 30% lower.

In summary, we report a limit on the production cross section of the standard-model Higgs boson in association with a vector boson $V = W, Z$ with hadronic decays. Tighter limits are being obtained in the semileptonic decay channels. However, this is the first limit obtained in the difficult all-hadronic channel in Run II. We expect the analysis to be refined with time, and to be able to contribute to the overall Tevatron information on light Higgs production when all data of the Tevatron Run II have been analyzed.

We thank the Fermilab staff and the technical staffs of the participating institutions for their vital contributions. This work was supported by the U.S. Department of Energy and National Science Foundation; the Italian Istituto Nazionale di Fisica Nucleare; the Ministry of Education, Culture, Sports, Science and Technology of Japan; the Natural Sciences and Engineering Research

TABLE I: Number of predicted standard-model Higgs boson signal events and expected and observed 95% confidence level upper limits on the VH production cross section, expressed as a multiple of the standard model cross section for several Higgs boson masses. The final column shows the observed limit on the cross section in pb .

M_H (GeV/c^2)	SM VH N	Expected lim. ($\sigma/\sigma_{\text{SM}}$)	Obs. lim. ($\sigma/\sigma_{\text{SM}}$)	Obs. lim. (pb)
100	7.2	$28.7^{+12.7}_{-8.4}$	29.7	13.9
105	6.6	$33.7^{+14.8}_{-9.9}$	37.6	14.9
110	6.4	$36.6^{+15.8}_{-11.2}$	38.7	13.2
115	5.5	$36.8^{+16.3}_{-10.4}$	37.5	11.0
120	5.2	$39.6^{+16.8}_{-12.2}$	38.2	9.66
125	4.2	$46.8^{+20.2}_{-14.3}$	43.4	9.51
130	3.5	$53.6^{+22.9}_{-15.6}$	48.0	9.13
135	2.6	$80.2^{+34.1}_{-23.2}$	73.6	12.2
140	2.0	$115^{+51.7}_{-35.9}$	107	15.5
145	1.3	$176^{+81.0}_{-52.7}$	163	20.7
150	0.86	$287^{+127}_{-87.8}$	261	28.9

Council of Canada; the National Science Council of the Republic of China; the Swiss National Science Foundation; the A.P. Sloan Foundation; the Bundesministerium für Bildung und Forschung, Germany; the Korean Science and Engineering Foundation and the Korean Research Foundation; the Science and Technology Facilities Council and the Royal Society, UK; the Institut National de Physique Nucléaire et Physique des Particules/CNRS; the Russian Foundation for Basic Research; the Comisión Interministerial de Ciencia y Tecnología, Spain; the European Community's Human Potential Programme; the Slovak R&D Agency; and the Academy of Finland.

-
- [1] P. W. Higgs, Phys. Rev. Lett. **13**, 508 (1964).
 - [2] F. Englert and R. Brout, Phys. Rev. Lett. **13**, 321 (1964).
 - [3] R. Barate et al. (LEP Working Group for Higgs boson searches), Phys. Lett. **B565**, 61 (2003).
 - [4] J. Alcaraz et al. (LEP-Tevatron-SLD Electroweak Working Group) (2006), hep-ex/0612034.
 - [5] LEP-Tevatron-SLD Electroweak Working Group (2008), arXiv:0811.4682.
 - [6] A. Djouadi, J. Kalinowski, and M. Spira, Comput. Phys. Commun. **108**, 56 (1998).
 - [7] T. Aaltonen et al. (CDF Collaboration), Phys. Rev. D **78**, 032008 (2008).
 - [8] T. Aaltonen et al. (CDF Collaboration), Phys. Rev. Lett. **101**, 121801 (2008).
 - [9] C. Amsler et al. (Particle Data Group), Phys. Lett. **B667**, 1 (2008).
 - [10] F. Abe et al. (CDF Collaboration), Phys. Rev. Lett. **81**, 5748 (1998).
 - [11] J. Valls and R. Vilar, FERMILAB-CONF-99-163-E (1998).
 - [12] D. Acosta et al. (CDF Collaboration), Phys. Rev. D **71**,

- 032001 (2005).
- [13] A. Abulencia et al. (CDF Collaboration), *J. Phys. G* **34**, 2457 (2007).
 - [14] T. Aaltonen et al. (CDF Collaboration) (2008), arXiv:0811.1062.
 - [15] CDF uses a cylindrical coordinate system with the z axis along the proton beam direction. Pseudorapidity is $\eta \equiv -\ln(\tan \theta/2)$, where θ is the polar angle, and ϕ is the azimuthal angle relative to the proton beam direction, while transverse momentum $p_T = |p| \sin \theta$, and transverse energy $E_T = E \sin \theta$.
 - [16] T. Sjostrand et al., *Computer Phys. Commun.* **135**, 238 (2001).
 - [17] E. Gerchtein and M. Paulini (2003), physics/0306031.
 - [18] F. Abe et al. (CDF Collaboration), *Phys. Rev. D* **45**, 1448 (1992).
 - [19] A. Bhatti et al., *Nucl. Instrum. Methods A* **566**, 375 (2006).
 - [20] A. Abulencia et al. (CDF Collaboration), *Phys. Rev. D* **74**, 072006 (2006).
 - [21] A. Abulencia et al. (CDF Collaboration), *Phys. Rev. D* **74**, 032009 (2006).
 - [22] J. Pumplin et al., *J. High Energy Phys.* **012**, 0207 (2002).
 - [23] M. L. Mangano et al., *J. High Energy Phys.* **0307**, 001 (2003).
 - [24] J. Alwall et al., *J. High Energy Phys.* **0709**, 028 (2007).
 - [25] T. Junk, *Nucl. Instrum. Methods A* **434**, 435 (1999).